Original paper

Dental Materials Journal 19(1) : 34−49, 2000

Corrosion Characteristics of Ferric and Austenitic Stainless Steels for Dental Magnetic Attachment

Kazuhiko ENDO, Masahiro SUZUKI and Hiroki OHNO

Department of Dental Materials Science, School of Dentistry,
Health Sciences University of Hokkaido
1757 Kanazawa, Ishikari-tobetsu, Hokkaido 061-0293, Japan

Received October 15, 1999/Accepted December 9, 1999

The corrosion behaviors of four ferric stainless steels and two austenitic stainless steels were examined in a simulated physiological environment (0.9% NaCl solution) to obtain basic data for evaluating the appropriate composition of stainless steels for dental magnetic attachments. The corrosion resistance was evaluated by electrochemical techniques and the analysis of released metal ions by atomic absorption spectrophotometry. The surface of the stainless steels was analyzed by X-ray photoelectron spectroscopy (XPS). The breakdown potential of ferric stainless steels increased and the total amount of released metal ions decreased linearly with increases in the sum of the Cr and Mo contents. The corrosion rate of the ferric stainless steels increased 2 to 6 times when they were galvanically coupled with noble metal alloys but decreased when coupled with commercially pure Ti. For austenitic stainless steels, the breakdown potential of high N-bearing stainless steel was approximately 500 mV higher than that of SUS316L, which is currently used as a component in dental magnetic attachments. The enriched nitrogen at the alloy/passive film interface may be effective in improving the localized corrosion resistance.

Key words : Stainless steels, Magnetic attachment, Corrosion resistance

INTRODUCTION

Dental magnetic attachments are increasingly used in overdentures and removable partial dentures due to the development of a small Nd-Fe-B magnet with high intrinsic coercivity[1]. Since the corrosion resistance of rare earth magnets is quite low[2], the magnet is encapsulated in a cup yoke made of ferric and austenitic stainless steels. Typical denture retention systems currently employed consist of an encapsulated magnet embedded in the denture and a ferric stainless steel keeper embedded in the noble metal alloy root cap by cast bonding[3]. High corrosion resistance and excellent magnetic properties are required for the stainless steels used in both the cup yoke and keeper.

At present, the stainless steels used for magnetic attachments are selected from among steels manufactured for engineering purposes. Takada and Okuno examined the corrosion behaviors of stainless steels currently employed in dental magnetic attachment systems and suggested that SUS444 and SUS447J1 can be used clinically like SUS316L, which has long been used in orthopedic and dental implants for fracture fixation and joint replacement[4]. To develop a new stainless steel specific to dental

magnetic attachments, however, the relationship between alloy composition and corrosion resistance as well as magnetic properties must be examined in detail. The influence of alloy composition on the corrosion resistance of stainless steels, however, has not been systematically investigated in simulated physiological environments.

The present study examined the corrosion behaviors of six ferric stainless steels with different compositions in a simulated physiological environment to obtain basic data for evaluation of the appropriate composition of stainless steels for dental magnetic attachments. The galvanic corrosion of the ferric stainless steels encountered when the keeper is embedded in a root cup made of a noble metal alloy or screwed into implant abutments made of commercially pure Ti was assessed electrochemically. In addition to ferric stainless steels, the corrosion behavior of a high-N bearing austenitic stainless steel with extremely low Ni content was examined and compared with that of SUS316L to develop a dental attachment system which can be used for patients with Ni hypersensitivity. The influence of nitrogen on the corrosion resistance was also investigated.

MATERIALS AND METHODS

Materials

Two austenitic and six ferric stainless steels were employed in this study. The chemical compositions of the stainless steels are shown in Table 1; SUS316L is an austenitic stainless steel which has long been used in orthopedic implants for fracture fixation and joint replacement. This stainless steel has also been used in dentistry for orthodontic appliances, as a miniplate for jaw fixation, and in magnetic attachments. Eu-90 is a high-N bearing austenitic stainless steel with an Ni content as low as 0.12%. This steel was experimentally manufactured by VSG Energie und Schmiedetechnik GmbH (Germany) as a round robin test specimen used to elucidate the role of nitrogen in improving the mechanical properties and corrosion resistance of austenitic stainless steels. The ferric stainless steels were six commercially available stainless steels with different Cr and Mo contents. The carbon and nitrogen contents were below 0.02% in all the steels to decrease the susceptibility to intergranular corrosion

Table 1 Chemical compositions of austenitic and ferric stainless steels (mass%)

Designation		C	Si	Mn	P	Ni	Cr	Mo	Cu	Nb	N	Ti	Fe
Austenitic stainless steels	SUS316L	0.023	0.36	0.92	0.031	12.15	16.47	2.03	–	–	0.046	–	bal
	Eu-90	0.050	0.97	16.66	0.020	0.12	15.62	3.83	–	–	0.810	–	bal
Ferric stainless steels	SUS430	0.008	0.56	0.30	0.026	0.18	17.51	0.07	0.06	–	0.007	0.24	bal
	U-4	0.016	0.40	0.37	0.026	0.15	18.45	0.50	0.09	0.37	0.016	–	bal
	U-2	0.006	0.57	0.21	0.023	0.14	18.16	2.06	0.05	0.25	0.015	–	bal
	U-22	0.003	0.48	0.21	0.033	0.22	21.91	1.99	0.09	0.13	0.008	–	bal
	U-20	0.003	0.15	0.13	0.024	0.18	27.18	3.52	0.06	0.16	0.008	–	bal
	SUS447J	0.003	0.17	0.08	0.020	0.17	29.75	2.03	–	–	0.007	–	bal

Table 2 Chemical compositions of noble metal alloys (mass%)

Noble metal alloys	Au	Ag	Pd	Pt	Cu	others
Ag-Pd-Cu-Au alloy	12	55	20	–	10	3
ADA Type Ⅳ Au alloy	70	8	3	2	16	1

due to the precipitation of Cr carbide and/or Cr nitride at the grain boundaries[5].

Two noble metal alloys and commercially pure Ti (CPTi) were employed for the galvanic corrosion tests. Table 2 shows the chemical compositions of the two noble metal alloys, Ag-Pd-Cu-Au alloy and ADA type Ⅳ Au alloy.

Specimens of 12 × 12 × 1 mm^3 were cut from the stainless steels and commercially pure Ti plates received from the manufacturer. Noble metal alloy specimens were cast in 12 × 12 × 1 mm^3 by conventional dental casting techniques. After casting, the alloy specimens were bench-cooled to room temperature in an investment. All specimens were polished mechanically to a mirror finish using emery papers followed by 0.05μm alumina pastes. The polished specimens were cleaned ultrasonically in distilled water for 60 s and then dried with flowing air.

Potentiodynamic polarization measurements

Potentiodynamic polarization measurements were carried out in 0.9% NaCl solution at 37℃. The solution was deaerated with ultrapure Ar gas before and during the measurements. Before starting the potential scan, the specimens were cathodically treated in the solution under a constant current density of $-10\mu A \cdot cm^{-2}$ for 300 s to remove the preformed oxide film in air. The potentiodynamic measurements were started from −1000 mV (vs. Ag/AgCl reference electrode) at a scan rate of 0.17 $mV \cdot s^{-1}$. The measurements were repeated three times using different specimens for each stainless steel.

Immersion test

The amounts of Fe, Cr, Mo, Ni, and Mn ions released into solution from the stainless steel specimens were determined by atomic absorption spectrophotometry (5100 ZL, Perkin Elmer, Norwalk, U.S.A.). The polished plate specimens were immersed in 20 ml polystyrene vials containing 10 ml of 0.9% NaCl solution at 37℃. After immersion for 7 days, the specimens were removed and these first sample solutions were immediately acidified by the addition of 1 ml of 1 M HNO_3 solution. The HNO_3 and Cl ion concentrations of the standard solutions were identical to those of the sample solutions, and a graphite tube atomizer was employed for the analysis of all metal ions. After removal of the first sample solution, the specimens were rinsed with distilled water, and immersed in freshly prepared 0.9% NaCl solution. After subsequent immersion for 14 days, the second sample solutions were acidified and analyzed in the same way as the first sample solutions. Four specimens were prepared and tested for each stainless steel.

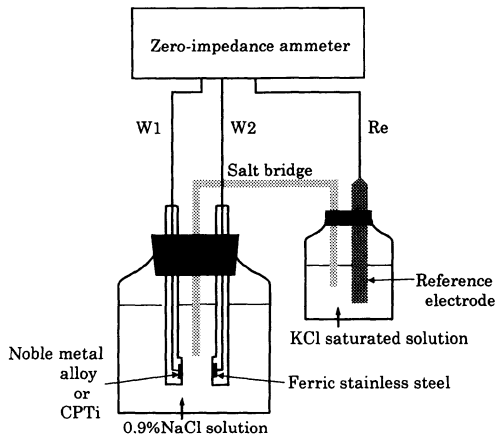

Fig. 1 The instrumentation setup for measuring the galvanic current.

Galvanic corrosion tests

The corrosion potentials (Ecorr) of the stainless steels, CPTi, and noble metal alloys in a 0.9% NaCl solution were measured for 48 hours using an electrometer having an input impedance of $10^{12}\Omega$. The galvanic current between the stainless steels and CPTi or noble metal alloys was monitored for 48 hours by a zero-impedance ammeter. Fig. 1 shows the instrumentation setup for measuring the galvanic current. Two different specimens were mounted each in a specimen holder which limited the surface area of the specimen to 1 cm^2. The distance between the two specimens was approximately 2 cm. The two specimens were electrically connected through a zero-impedance ammeter (2090, Toho Technical Research, Tokyo, Japan) and the galvanic current was recorded up to 48 hours. The measurements were carried out three times for each galvanic couple. This experiment was carried out only for the ferric stainless steels.

Surface analysis by XPS

The surface of the Eu-90 specimen was characterized by X-ray photoelectron spectroscopy (XPS) after immersion in 0.9% NaCl solution for 7 days to examine the chemical states of nitrogen at the surface. The XPS spectra were obtained using an X-ray photoelectron spectrometer (ESCA-850, Shimadzu Co. Ltd., Kyoto, Japan) with Al K_α radiation operated at a 7 kV accelerating voltage and 30 mA current under a vacuum of 1×10^{-6} Pa. The binding energy scale was calibrated by the Au $4f_{7/2}$ and Cu $2p_{3/2}$ peaks at 83.8 and 932.8 eV, respectively. The passive film on Eu-90 was subjected to Ar^+ etching at 2 kV and 20 mA under a pressure of 5×10^{-4} Pa in the spectrometer. The etching rate on pure Ag was approximately 0.05 nm $\cdot$ s^{-1} under these conditions.

RESULTS

Potentiodynamic polarization behavior

Fig. 2 shows typical potential/current density curves for the six ferric stainless steels in deaerated 0.9% NaCl solution. The passive potential region of the ferric stainless steels increased with increases in Cr content. The breakdown potential of U-2, which contains 2.06% of Mo, was +100 mV higher than that of U-4. Since the Cr contents of U-2 and U-4 were very similar, it may be concluded that the addition of Mo was effective in increasing localized corrosion resistance in the 0.9% NaCl solution. The U-20 and SUS447J contained more than 30% Cr and Mo, and their breakdown potentials were above +1000 mV (vs. Ag/AgCl reference electrode). In the transpassive region, both the dissolution reaction of the Cr-rich oxide film and the oxygen evolution reaction could proceed simultaneously over the entire exposed surface. No localized corrosion was observed on U-20 and SUS447J after the polarization measurements.

Fig. 3 shows typical potential/current density curves for the two austenitic stainless steels. The breakdown potential for SUS 316L was +310 mV, and corrosion progressed with highly localized pitting above the breakdown potential. The breakdown potential for Eu-90 was +860 mV, which is approximately 500 mV higher than that for SUS316L. Above this potential, transpassive dissolution of the Cr-rich oxide film proceeded uniformly over the entire exposed surface. These results demonstrate that the localized corrosion resistance of Eu-90 was significantly higher than that of SUS316L in 0.9% NaCl solution. Since the Cr and Mo contents of Eu-90 are similar to those in SUS316L, this remarkably high breakdown potential for Eu-90 was attributed to the small amounts of nitrogen contained.

Amount of released metal ions

Table 3 shows the amount of Fe, Cr, Mo, Mn, and Ni ions released into the 0.9% NaCl solution during 7 days of immersion. The values in the table represent averages

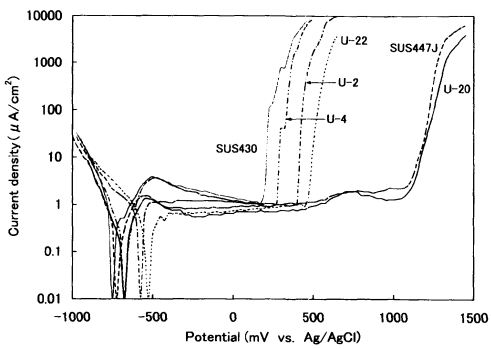

Fig. 2 Potential/current density curves of the six ferric stainless steels in deaerated 0.9% NaCl solution at 37℃.

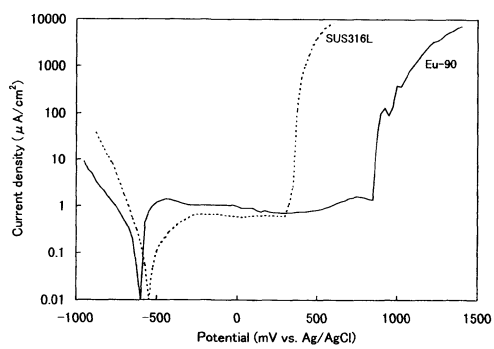

Fig. 3 Potential/current density curves of the two austenitic stainless steels in deaerated 0.9% NaCl solution at 37℃.

Table 3 Amounts of metal ions released from the austenitic and ferric stainless steels during 7 days of immersion ($ng \cdot cm^{-2}$)

Designation	Fe	Cr	Mo	Mn	Ni
SUS316L	391.6 (27.1)	10.2 (1.8)	14.5 (2.4)	−	63.1 (4.1)
Eu-90	241.3 (30.0)	13.5 (0.7)	15.4 (2.3)	233.8 (14.6)	−
SUS430	484.6 (68.5)	9.9 (2.0)	−	−	−
U-4	413.3 (43.3)	10.2 (2.5)	1.0 (1.0)	−	−
U-2	460.9 (89.9)	10.7 (2.3)	14.4 (4.6)	−	−
U-22	361.1 (84.6)	8.5 (0.7)	7.3 (2.1)	−	−
U-20	175.8 (64.2)	8.0 (1.2)	11.8 (2.5)	−	−
SUS447J	152.0 (39.7)	5.9 (1.0)	6.1 (0.9)	−	−

( ): S.D. − : not detected

Table 4 Amounts of metal ions released from the austenitic and ferric stainless steels from the 8th days to the 21st day ($ng \cdot cm^{-2}$)

Designation	Fe	Cr	Mo	Mn	Ni
SUS316L	56.9 (16.9)	−	−	−	23.4 (2.2)
Eu-90	9.2 (1.5)	−	−	22.0 (2.1)	−
SUS430	62.6 (8.1)	−	−	−	−
U-4	64.9 (17.7)	−	−	−	−
U-2	63.0 (8.9)	−	−	−	−
U-22	54.3 (10.1)	−	−	−	−
U-20	41.5 (16.2)	−	−	−	−
SUS447J	34.7 (3.8)	−	−	−	−

( ): S.D. − : not detected

for four samples and the standard deviations are shown in parentheses. The dominant corrosion product for both austenitic and ferric stainless steels was Fe ions. The amount of released Fe ions generally decreased with increasing Cr content of the steels in 0.9% NaCl solution. The amount of Fe ion released from the Eu-90, however, was significantly lower than that could be expected from the Cr and Mo contents but as much Mn as Fe was released. The amount of Ni ions released from SUS316L was 63.1 $ng \cdot cm^{-2}$, which was approximately 1/6 of the released Fe ions. Cr and Mo ions were detected in the solutions from all stainless steels but their concentrations were mostly one order of magnitude or more lower than those of Fe ions. For the ferric stainless steels, the amounts of Ni and Mn ions were below the detection limit.

Table 4 shows the amounts of metal ions released into the solution from the 8 th day to the 21st day. The amounts of released Fe ions for both austenitic and ferric stainless steels were much lower than those released during the first 7 days. The Mn ions were released preferentially from Eu-90 and the amount of Mn was twice that of

Fe ions. In addition to Fe ions, small amounts of Ni ions were released from SUS316L. With the ferric stainless steels, no metal ions other than Fe ions were detected in the second sample solutions (8 to 21 days).

Galvanic corrosion behavior

Fig. 4 show the variations in the corrosion potential of the ferric stainless steels, the two noble metal alloys, and CPTi with time in 0.9% NaCl solution. With time, the corrosion potentials of the stainless steels and CPTi moved in the noble direction due to the formation of the more protective films in the solution. The corrosion potentials of the two noble metal alloys also moved in the noble direction, probably due to the enrichment of the Au and Pd at the surface after the preferential dissolution of Ag and Cu ions into the solution. The Type Ⅳ Au alloy was the most noble followed by the Ag-Pd-Cu-Au alloy, the ferric stainless steels, and CPTi.

Fig. 5 shows the variations in galvanic current density with time for galvanic couples of ferric stainless steels with the Type Ⅳ Au alloy in 0.9% NaCl solution. As predicted from the corrosion potentials for these alloys, ferric stainless steel was anodic to the Au alloy when the two alloys were galvanically coupled. The galvanic current density was initially high but rapidly decreased and reached about 10 nA · cm^{-2} after several hours. Similar results were obtained for the galvanic couples of ferric stainless steels with the Ag-Pd-Cu-Au alloy (Fig. 6). Fig. 7 shows the galvanic current density versus time for the galvanic couples of ferric stainless steels with CPTi. The ferric stainless steels showed more noble corrosion potentials than CPTi and they were cathodic to CPTi. The galvanic current densities decreased continuously with time and had not reached the steady-state values after 48 hours, due to the continuous increase in the corrosion potential of CPTi shown in Fig. 4.

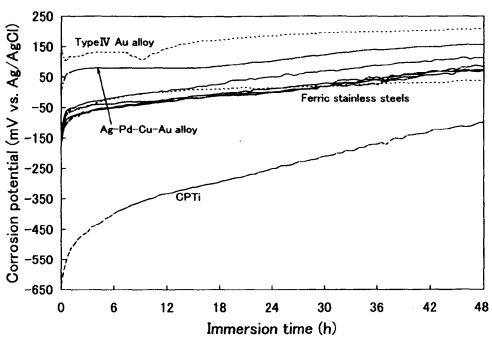

Fig. 4 Variations in the corrosion potential of the ferric stainless steels, the two noble metal alloys, and CPTi in 0.9% NaCl solution.

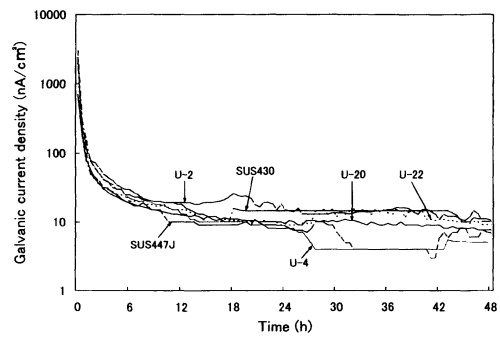

Fig. 5 Variations in the galvanic current density with time for galvanic couples of the ferric stainless steels with the Type Ⅳ Au alloy in 0.9% NaCl solution.

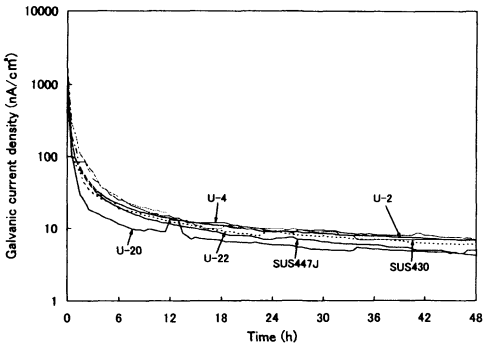

Fig. 6 Variations in the galvanic current density with time for galvanic couples of the ferric stainless steels with the Ag-Pd-Cu-Au alloy in 0.9% NaCl solution.

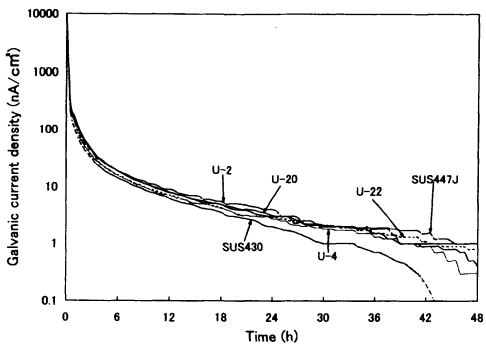

Fig. 7 Variations in the galvanic current density with time for galvanic couples of the ferric stainless steels with CPTi in 0.9% NaCl solution.

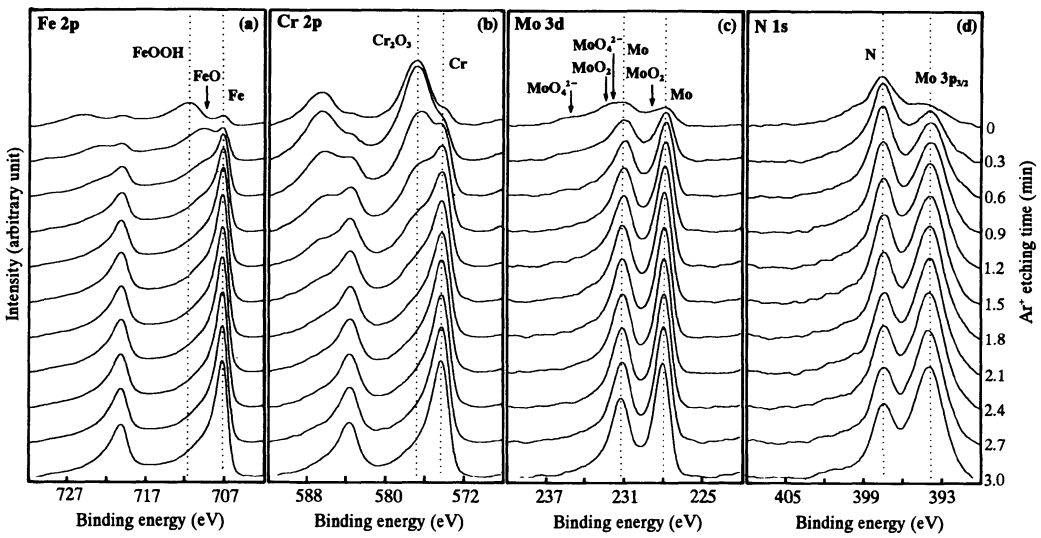

Fig. 8 XPS spectra as a function of Ar^+ etching time from the Eu-90 surface after immersion in 0.9% NaCl solution for 7 days; (a) Fe 2p, (b) Cr 2p, (c) Mo 3d, (d) N 1s

Surface analysis of the high-N bearing austenitic stainless steel

Fig. 8 shows the Fe 2p (a), Cr 2p (b), Mo 3d (c), and N 1s(d) spectra obtained from the Eu-90 surface after immersion in 0.9% NaCl solution for 7 days, as a function of Ar^+ etching time. The Fe 2p and Cr 2p spectra demonstrate that the passive film on Eu-90 was mainly composed of Cr-rich oxide film while FeOOH was present in the outer part of the passive film. At 1.8 min of Ar^+ etching, the Cr 2p peak at 576.8 eV corresponding to Cr_2O_3 disappeared, indicating that the passive film on the alloy was completely removed. The Mo 3d spectra suggest that Mo was present in the metallic

and the oxidized states at the surface. After Ar^+ etching for 0.3 min, the peaks corresponding to the Mo^{4+} and Mo^{6+} states almost disappeared, indicating that the both MoO_2 and MoO_4^{2-} were present in the outer part of the passive film as was FeOOH. The N 1s spectrum from the unetched surface showed several peaks on both the higher and lower binding energy sides of the main peak at 397.7 eV. This main peak was attributed to atomic nitrogen dissolved in Eu-90. The intensity of the peak at 393.8 eV increased with increases in Ar^+ etching time, and this peak could be assigned to the Mo $3p_{3/2}$ peak corresponding to the metallic Mo dissolved in the alloy[6]. Since the Mo $3p_{3/2}$ line overlaps the N 1s line, curve fittings for multiple peaks in the spectrum obtained from the unetched surface were performed based on the reported binding energies of N 1s and Mo $3p_{3/2}$ spectra for different chemical states[7,8], and the results are shown in Fig. 9. The intensities of the N 1s peaks corresponding to NH_3, NH_4^+, and CrN decreased rapidly with Ar^+ etching. The detected compounds of NH_3 and NH_4^+ were not reaction products of nitrogen dissolved in the alloy and protons in the solution but contaminants adsorbed on the surface as reported elsewhere[8]. The $3p_{3/2}$ peak corresponding to MoO_4^{2-} completely overlapped the N 1s peak corresponding to the atomic nitrogen, and these two peaks could not be separated each other. The reported binding energy position of Cr_2N is 397.5 eV, which is almost identical to that of atomic nitrogen. This fact suggests that Cr-rich nitride may also be present at the

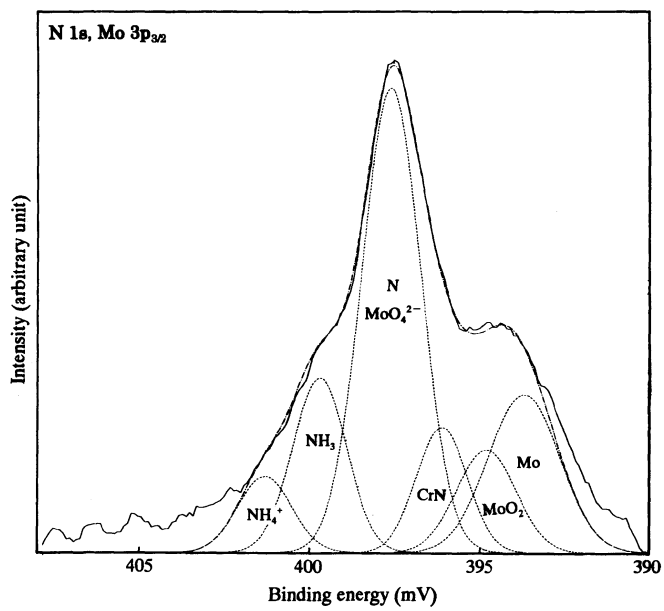

Fig. 9 N 1s spectrum from the unetched Eu-90 surface after immersion in 0.9% NaCl solution for 7 days. Solid line: measured spectrum, dotted line: separated component spectrum, chained line: sum of component spectra.

alloy surface after immersion in 0.9% NaCl solution.

DISCUSSION

Localized corrosion resistance of stainless steels

It is well known that Cr is the crucial element in the passivity of stainless steels and 2 to 3 mass% of Mo enhances resistance to pitting corrosion in chloride containing environments[11]. Here, the localized corrosion resistance of the stainless steels in a simulated physiological environment is discussed quantitatively in relation to the Cr and Mo contents.

Fig. 10 shows the relationship between the total amount of Cr and Mo contained in each stainless steel (Cr · Mo content) and the breakdown potential in deaerated 0.9% NaCl solution. The breakdown potential, E_b, for ferric stainless steels increases linearly with increases in Cr · Mo content. The regression line obtained from the data for the ferric stainless steels is as follows;

$$E_b = 61 \times (\mathrm{Cr} \cdot \mathrm{Mo})\ \mathrm{mass\%} - 849\ (\mathrm{mV}) \quad (1)$$

Corrosion tests previously conducted in acid solutions containing chloride ions or 10% $FeCl_3$ solution suggested that 1% Mo increases the pitting potential of stainless steels equivalent to approximately 3.3% of Cr[12]. According to equation (1), the effect of Mo in increasing the breakdown potential is identical to that of Cr. The effect of Mo may have been lower in the 0.9% NaCl solution employed in the present study than in more severe corrosion environments like acidic chloride or $FeCl_3$ solutions.

The breakdown potential for a ferric stainless steel in a simulated physiological environment can be estimated by equation (1) from the Cr and Mo contents. This equation is useful in evaluating the composition of ferric stainless steels specific to

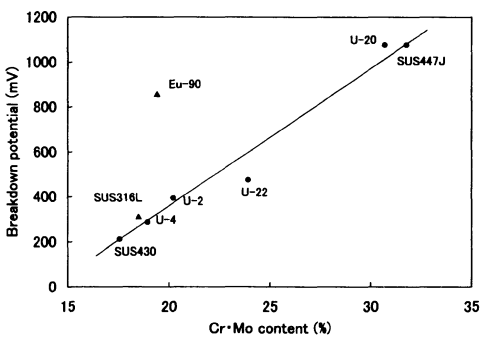

Fig. 10 The relationship between the sum of Cr and Mo contents in each stainless steel and the breakdown potential in deaerated 0.9% NaCl solution. The regression line was obtained from the data for the ferric stainless steels.

dental magnetic attachments.

Equation (1) also holds for austenitic stainless steels as the breakdown potential for SUS316L is accurately estimated by the equation. The breakdown potential for Eu-90, however, was approximately 500 mV higher than that expected from equation (1). Previous studies have shown that the nitrogen added to austenitic stainless steels improves their localized corrosion resistance in chloride environments[9,10]. The enhanced passivity for Eu-90 demonstrated in this study was attained by the addition of a small amount of nitrogen to the alloy. The measured breakdown potential for Eu-90 indicates that 1% of nitrogen in austenitic stainless steels increases the breakdown potential equivalent to approximately 10% of Cr. The role of nitrogen in increasing pitting corrosion resistance will be discussed later.

Dissolution behavior of stainless steels

Fig. 11 shows the variation in the total amount of metal ions released into the solution versus the Cr · Mo content for both ferric and austenitic stainless steels. In the first 7 days, the amount of released metal ions (solid circles) decreased linearly with increases in Cr · Mo content. This result suggests that the resistance of stainless steels to general corrosion in 0.9% NaCl solution was also increased by increasing the Cr · Mo content.

The average dissolution rate of metal ions after 7 days (solid triangles) was much lower than the initial dissolution rate, and it was almost independent of the Cr · Mo content. With the preferential dissolution of Fe ions, a Cr-rich oxide film grew on the specimen, and this passive film, aged in the solution, was responsible for the increased resistance to general corrosion especially for the stainless steels with low Cr · Mo content. The initial dissolution rate was maintained in the presence of fretting and friction[13], suggesting that the initial resistance to general corrosion may

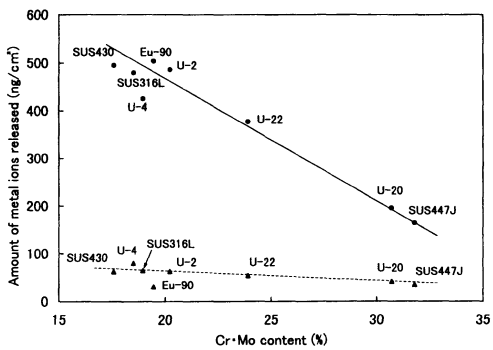

Fig. 11 The relationship between the sum of Cr and Mo contents in each stainless steel and the amount of metal ions released into 0.9% NaCl solution. ● first sample solution, ▲ second sample solution

be more important when the dissolution behavior of dental magnetic attachments in the service condition is considered.

The localized corrosion resistance of Eu-90 was much higher than that of SUS316L while the general corrosion resistance estimated from the amount of released metal ions was identical for both these austenitic stainless steels. For high-N bearing austenitic stainless steels without Ni, Mn is essential element to increase the concentration of dissolved nitrogen. The Mn is electrochemically the most active element among the metals in stainless steels and the amount of released Mn ions during the first 7 days was as high as that of Fe ions. After 7 days, Mn ions were the dominant corrosion product released into the solution. Therefore, the Mn content must be minimized to develop a Ni-free austenitic stainless steel which is highly resistant to both general and localized corrosion.

Galvanic corrosion behavior of the ferric stainless steels

When the ferric stainless steels were galvanically coupled with Type IV Au alloy or Ag-Pd-Cu-Au alloy, all the stainless steels were anodic to the noble metal alloys. The galvanic current densities, however, decreased to approximately 10 nA · cm^{-2} after several hours and there were no significant differences in the galvanic current densities of the ferric stainless steels investigated in this study. The corrosion rate of uncoupled ferric stainless steels in 0.9% NaCl solution could be approximately estimated from the amount of metal ions released into the solution, ΔW(g · cm^{-2}), using Faraday's law,

$$i_{corr}=\frac{nF}{T}\left\{\frac{\Delta W_{Fe}}{M_{Fe}}+\frac{\Delta W_{Cr}}{M_{Cr}}+\frac{\Delta W_{Mo}}{M_{Mo}}\right\} \quad (2)$$

where n is the number of electrons exchanged in the dissolution reactions; T, M and F are the test period, atomic weight, and the Faraday constant, respectively. In this calculation, the oxidation states of the Fe and Mo ions were assumed to be divalent, and Cr ions to be trivalent. The average corrosion rate over the test period (7 days) thus estimated was 1−3 nA · cm^{-2}. Comparing these estimated corrosion rates with the steady-state values of the measured galvanic current density (10 nA · cm^{-2}), the corrosion rate was found to be increased approximately 3 times for SUS430 and 10 times for SUS447J when the specimens were galvanically coupled with noble metal alloys. It is desirable to insulate the stainless steel keeper from the cast root cup made of a noble metal alloy to minimize the corrosion of the stainless steel in the oral environment. Takada also pointed out that this insulation is essential when the surface area of the root cup is much larger than that of a stainless steel keeper[14].

The ferric stainless steels were cathodic to CPTi and their corrosion rate was retarded when they were galvanically coupled with CPTi. The galvanic current density measured at 48 hours was approximately 1 nA · cm^{-2} , which was one order of magnitude lower than that observed between stainless steel and noble metal alloy. The corrosion potential of CPTi, however, continuously moved in the noble direction up to 48 hours (Fig. 4). After 48 hours, the ferric stainless steels would be anodic to CPTi,

and if so the corrosion rate of the ferric stainless steels would increase. A long-term study would be necessary to appropriately evaluate the galvanic corrosion encountered when keepers made of a ferric stainless steel are screwed into the implant abutments made of CPTi.

Role of nitrogen in improving the localized corrosion resistance of austenitic stainless steels

Previous studies have demonstrated surface enrichment of nitrogen on the N-containing austenitic stainless steels by XPS and Auger electron spectroscopy. Different results, however, have been reported so far[12]. For example, nitrogen was enriched on the surface of oxide in 0.1M NaCl solution[15] while it segregated to the metal-oxide interface during passivation in 0.1M HCl+0.4M NaCl solution[9] and in 0.5M H_2SO_4[16]. The reason for these different results may be that the exact location and chemical state of the enriched nitrogen at the surface change with alloy composition and environment. The XPS spectra obtained from the Eu-90 specimen after immersion in 0.9% NaCl solution were further analyzed to specify the location and chemical state of nitrogen at the surface and to discuss its effects in improving the localized corrosion.

Fig. 12 shows the variations in the intensities of the N 1s peak at 397.7 eV and the Mo $3p_{3/2}$ peak at 394.0 eV with Ar^+ etching time. As described in the results section, the peak intensity for N 1s at the unetched surface was slightly overestimated because of the overlapping Mo $3p_{3/2}$ peak corresponding to MoO_4^{2-}. From the Cr 2p spectra shown in Fig. 8 (b), it may be assumed that the passive film was almost removed after 1.8 min of Ar^+ etching. This assumption is supported by the fact that the peak intensity of the Mo $3p_{3/2}$ peak at 394.0 eV, corresponding to metallic Mo dissolved in the alloy, reached a constant value at 1.8 min. The intensity of the N 1s peak at 397.7 eV increased and reached a maximum at 0.9 min and then decreased, indicating

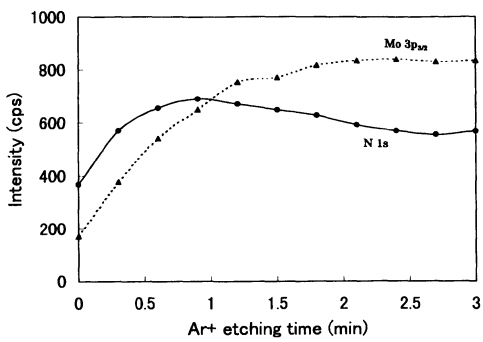

Fig. 12 Variations in the intensity for N 1s peak at 399.7 eV and Mo $3p_{3/2}$ peak corresponding to metallic Mo in the alloy with Ar^+ etching time.

that nitrogen was enriched at the inner part of the passive film near the passive film/alloy interface. The presence of atomic nitrogen in the film is unlikely and the enriched nitrogen may have been Cr-rich nitride incorporated in the film. Since the solubility of nitrogen in austenite is very low, part of the nitrogen segregated to the passive film/ alloy interface may form a Cr-rich nitride (Cr_2N). The fact that the binding energy position of Cr_2N is almost identical to that of atomic nitrogen supports this assumption[9,17]. Huang *et al.* also found Cr nitride in the passive film of the nitrogen and Mo containing laser cladded steels after immersion in 3.5% NaCl solution[7]. The intensity of the N 1s peak at 397.7 eV was higher after 1.8 min of Ar^+ etching than that obtained from the bulk alloy, suggesting that nitrogen was also enriched in atomic form at the alloy side of the interface.

The enriched nitrogen both in Cr-rich nitride and in atomic states may be effective in enhancing the passivity of Eu-90 in 0.9% NaCl solution. As suggested by Willenbruch *et al.*, the nitride layer formed at the inner part of the passive film may be stable and act as a reaction barrier to dissolution of the alloy[18]. The enriched atomic nitrogen may also prevent the growth of pits by the following mechanism. Once pitting corrosion is initiated, it is well known that an autocatalytic propagation of pitting occurs due to the concentrated hydrogen and chloride ions produced by the hydrolysis of metal chlorides in the pit[19]:

$$M^+Cl^- + H_2O \rightarrow MOH + H^+ + Cl^- \quad (3)$$

Osozawa and Okato suggested that the enriched nitrogen at the surface may react with H^+ ions to form NH_4^+ ions when the passive film is broken locally[20]:

$$N + 4H^+ + 3e \rightarrow NH_4^+ \quad (4)$$

As indicated by Fig. 13, this reaction inhibits a lowering of the pH in the initial pits. Thus the enriched nitrogen prevents growth of the initial pits and may thereby enhance repassivation. The extremely high breakdown potential for Eu-90 in 0.9% NaCl solution (Fig. 10) is considered to be attained by this buffer action of nitrogen concentrated at the passive film/alloy interface in the solution.

In addition to an extremely high resistance to localized corrosion, the Ni content of Eu-90 is only 0.12%. Since Ni is a strong hapten and is frequently involved in hypersensitivity reactions[21], a high-N bearing austenitic stainless steel free of Ni could

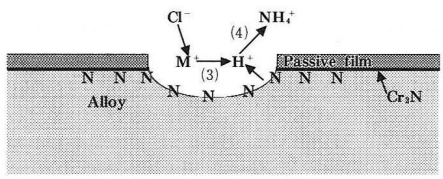

Fig. 13 Schematic model for inhibition of pit growth by the enriched nitrogen at the passive film/ alloy interface.

be a substitute for SUS316L, which is currently used as a component of dental magnetic attachments.

The composition of the ferric stainless steel specific to dental magnetic attachments should be determined based on both the corrosion resistance and the magnetic properties. A discussion of the magnetic properties of the six ferric stainless steels with different composition employed in this study is reported elsewhere[22].

CONCLUSIONS

The corrosion behaviors of six ferric stainless steels and two austenitic stainless steels were examined in 0.9% NaCl solution. The following results were obtained:

(1) The breakdown potential of ferric stainless steels increased linearly with increases in the sum of Cr and Mo contents (Cr · Mo), expressed as:

$$E_b = 61 \times (\mathrm{Cr} \cdot \mathrm{Mo})\ \mathrm{mass}\% - 849\ (\mathrm{mV})$$

(2) The breakdown potential of Eu-90 is approximately 500 mV higher than that expected from the Cr · Mo content. The protective layer of Cr-rich nitride formed at the inner part of the passive film and atomic nitrogen concentrated at the alloy surface may be responsible for this high localized corrosion resistance.

(3) The total amount of metal ions released from both ferric and austenitic stainless steels decreased linearly with increases in the Cr · Mo content.

(4) The corrosion rate of the ferric stainless steels increased 3 to 10 times when they were galvanically coupled with Type Ⅳ Au or Ag-Pd-Cu-Au alloys while the corrosion rate decreased when the ferric stainless steels were coupled with commercially pure Ti.

ACKNOWLEDGMENTS

The authors are grateful to Nippon Metal Industry Co. Ltd., Kawasaki Steel Corporation, and VSG Energie und Schmiedetechnik GmbH for supplying the experimental materials.

REFERENCES

1) Highton, R., Caputo, A. A., Pezzoli, M. and Matyas, J.: Retentive characteristics of different magnetic systems for dental applications, *J Prosthet Dent* **56** : 104-106, 1986.
2) Angelini, E., Pezzoli, M. and Zucchi, F.: Corrosion under static and dynamic conditions of alloys used for magnetic retention in dentistry, *J Prosthet Dent* **65** : 848-853, 1991.
3) Okuno, O., Ishikawa, S., Iimuro, F. T., Kinouchi, Y., Yamada, H., Nakano, T., Hamanaka, H., Ishihata, N., Mizutani, H. and Ai M.: Development of sealed yoke type dental magnetic attachment, *Dent Mater J* **10** : 172-184, 1991.
4) Takada, Y. and Okuno, O.: Corrosion behavior of stainless steels and dental precious alloys used for dental magnetic attachments, *J J Mag Dent* **3** : 14-22, 1994. (in Japanese)
5) Uhlig, H. H. and Revie, R. W.: Corrosion and Corrosion Control, 3rd ed., John Eiley & Sons, New York, 1985, pp.311-312.

6) Chastain, J. ed.: Handbook of X-ray photoelectron spectroscopy, Perkin-Elmer Co., Eden Prairie, 1992, pp.112-113.
7) Huang, C. C., Tsai, W. T. and Lee, J. T.: Electrochemical and surface studies on the passivity of nitrogen and molybdenum containing laser cladded alloys in 3.5 wt% NaCl solution, *Corros Sci* **37** : 769-780, 1995.
8) Endo, K., Abiko, Y., Suzuki, M., Ohno, H. and Kaku, T.: Corrosion resistance and biocompatibility of high nitrogen-bearing stainless steels, *Corrs Eng* **47** : 570-576, 1998.
9) Olefjord, I. and Wegrelius, L.: The influence of nitrogen on the passivation of stainless steels, *Corros Sci* **38** : 1203-1220, 1996.
10) Ohno, H., Tanabe, H., Sakai, A. and Misawa, T.: Pitting resistance and in-situ Raman study of nitrogen-compounds in a pit of high nitrogen-bearing austenitic stainless steels, *Corros Eng* **47** : 584-590, 1998. (in Japanese)
11) Atkinson, J. T. N. and VanDroffelaar, H.: Corrosion and its control, 1st ed., NACE, Houston, 1985, pp.176-179.
12) Osozawa, K.: The effects of nitrogen on the passivity and the pitting corrosion of stainless steels, *Corros Eng* **47** : 561-569, 1998. (in Japanese)
13) Syrett, B. C. and Wing, S. S.: An electrochemical investigation of fretting corrosion of surgical implant materials, *Corrosion* **34** : 379-386, 1978.
14) Takada, Y.: Corrosion of dental magnetic attachments and its prevention, *Dent Eng* **No.127** : 9-12, 1998. (in Japanese)
15) Lim, A. S. and Atrens, A.: ESCA studies of nitrogen-containing stainless steels, *Applied Physics* **A51** : 411-418, 1990.
16) Lu, Y. C., Bandy, R., Clayton, C. R. and Newman, R. C.: Surface enrichment of nitrogen during passivation of a highly resistant stainless steel, *J Electrochem Soc* **130** : 1774-1776, 1983.
17) Vanini, A. S., Audouard, J.-P. and Marcus, P.: The role of nitrogen in the passivity of austenitic stainless steels, *Corros Sci* **36** : 1825-1834, 1994.
18) Willenbruch, R. D., Clayton, C. R., Oversluizen, M., Kim, D. and Lu, Y.: An XPS and electrochemical study of the influence of molybdenum and nitrogen on the passivity of austenitic stainless steel, *Corros Sci* **31** : 179-190, 1990.
19) Fontana, M. G.: Corrosion engineering, 3rd ed., McGraw-Hill, New York, 1986, pp.63-69.
20) Osozawa, K. and Okato, N.: Effect of alloying elements,especially nitrogen, on the initiation of pitting in stainless steel, in Passivity and its breakdown on iron and iron based alloys, Staehle, R. W. and Okada, H., eds., NACE, Houston, 1976, pp.135-139.
21) Hildebrand, H. F., Veron, C. and Martin, P.: Nickel, chromium, cobalt dental alloys and allergic reactions: an overview, *Biomaterials* **10** : 545-548, 1989.
22) Suzuki, M., Endo, K. and Ohno, H.: Magnetic properties and susceptibility to intergranular corrosion of ferric stainless steels for dental magnetic attachment, *J Jpn Soc Dent Products* **13** : 43-50, 1999.